Available on CMS information server **CMS CR 2003/023**

CMS Conference Report

WCCM V - Fifth World Congress on Computational Mechanics, July 7-12, 2002, Vienna, Austria

Incorporation of Combined Experimental and FEA Results in FE-Models — with Application to CERN CMS Experiment

Michel LEBEAU*, Fr d ric MOSSIERE (Thomson Kraftanlagen),
Homayoon REZVANI NARAGHI

CERN, European Organization for Nuclear Research
CH-1211 Geneva 23, Switzerland
e-mail: Michel.Lebeau@cern.ch

Key words: experimental method, FEM, modelling, prototyping, structural analysis

Abstract

Results of FE-analyses and experimental tests were combined to determine parameters needed for the FE-simulation of complex loading conditions of a lightweight support structure within the CMS experiment, a high-performance, general-purpose particle detector to be commissioned in 2006 at CERN.

As a part of CMS the mechanical support of the 100 tons electromagnetic calorimeter (EB) consists of a hierarchy of modular structural components. At the EB medium modularity level, packages of Sub-Modules (assembly of composite alveolar structures with an aluminium cover containing high-density scintillating crystals) are accurately positioned in a quasi-built-in condition on a stiff aluminium support (Grid). The cantilever of the sub-modules is partly taken by a thin-walled aluminium container (Basket), which has to fulfil certain displacement, stress and stability criteria. An FE-model of the basket is rather easy to build, while the complex assembly of the sub-modules with the grid and the basket is difficult to simulate.

The first phase of the design resulted in a prototype support structure on which validation tests were performed. Following a design revision, which did not offer time for a complete re-modelling of the structure, it was decided to combine experimental data with limited FE-simulation.

a) Prototype sub-modules are connected together in packages and deformations measured for unsupported loading conditions
b) Prototype sub-module packages are connected to a Module container and deformations measured for the typical loading conditions
c) An FE-model only representing the container stiffness is built to compute deformations for the typical loading conditions
d) A combination of the above inputs taking inelastic displacement on account results in stiffness parameters for the sub-modules with respect to the relevant loading conditions, and thereby the transmitted forces to the basket

The determined load parameters were applied in the FE-model for the revised basket design in interaction with additional relevant load cases, and analyses were performed to validate the new design with respect to the above mentioned criteria.

1 Introduction

1.1 The CMS Electromagnetic Calorimeter Support Structure

CMS is a high-performance, general-purpose particle detector to be commissioned in 2006 at CERN, the European Laboratory for High Energy Particle Physics, based in Geneva, Switzerland (Fig.1.1.a).

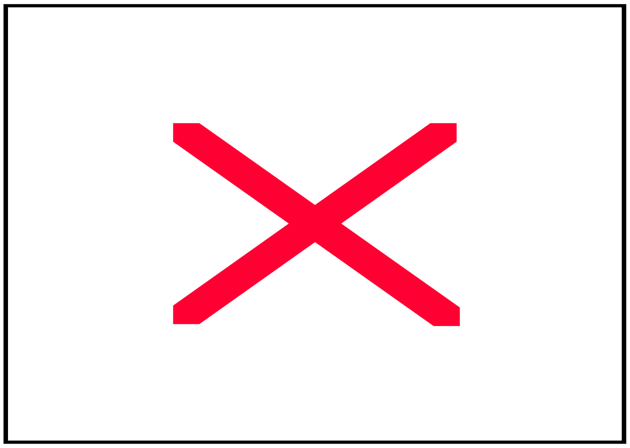

(a) General view of the CMS experiment

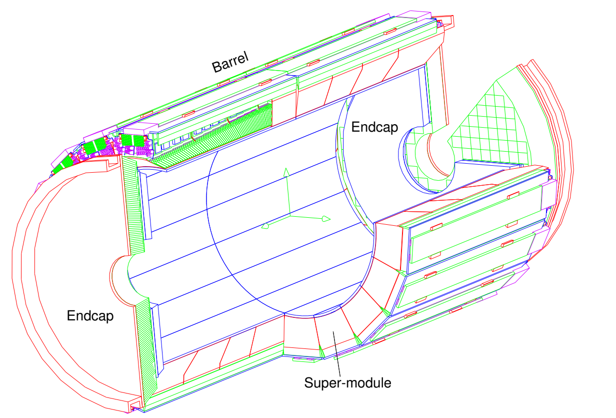

(b) The CMS Electromagnetic Calorimeter Barrel

Fig.1.1: The CMS experiment

As a part of CMS the mechanical support of the 100 tons Electromagnetic Calorimeter Barrel (EB) consists of a hierarchy of modular structural components, with major role to support and accurately position the detector active part consisting of 61200 pieces of high-density scintillating $PbWO_4$ crystals. The Barrel is divided into two half-barrels, each containing 18 Super-Modules displayed in circular symmetry (Fig.1.1.b).

Every super-module contains four Modules, held together by a long beam. In every module packages of Sub-Modules, assemblies of composite alveolar structures with an aluminium cover containing ten crystals (Fig.1.2.a) are accurately positioned in a quasi-built-in condition on a stiff aluminium support (Grid). The cantilever of the sub-modules is partly taken by a thin-walled aluminium container (Basket), which has to fulfil certain displacement, stress and stability criteria (Fig.1.2.b).

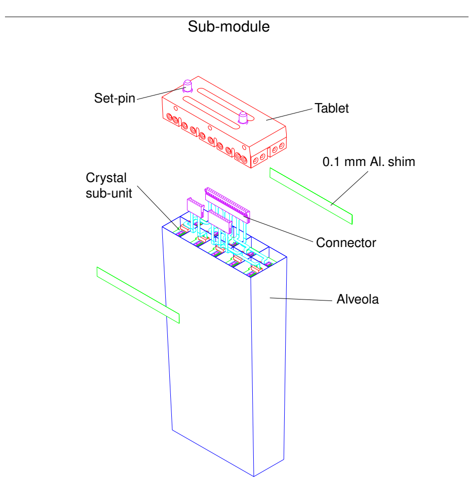

(a) The sub-module assembly

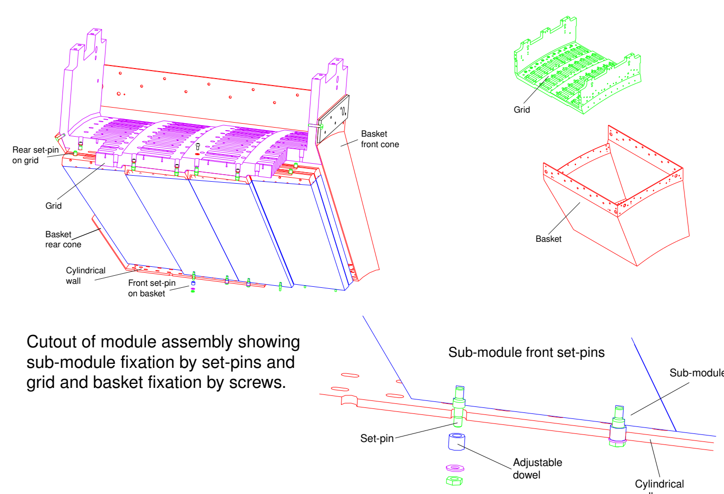

(b) The module assembly showing sub-modules connected to the grid and the basket

Fig.1.2: Modularity of the Calorimeter mechanical structure

1.2 The Support Structure Design Revision

The first phase of the design resulted in a prototype support structure on which validation tests were performed at the module scale on a Reduced Basket. Following a design revision, which did not give time for a full re-modelling of the structure, it was decided to combine experimental data with limited FE-simulation. The idea of the Super-Basket (Fig.1.3) was derived from the basket concept of the initial design as a robust and active structural element at super-module scale. The four separate baskets become a single structure: to four bottom plates corresponds now a single solid Cylindrical Wall of same thickness; the eight front and rear walls merge into one flat and four conical Webs: the two end webs keep same thickness as basket walls and the three intermediate webs merge the two initial walls. Basket side walls are cancelled because of their minor role and difficulty to accurately connect to the previous elements.

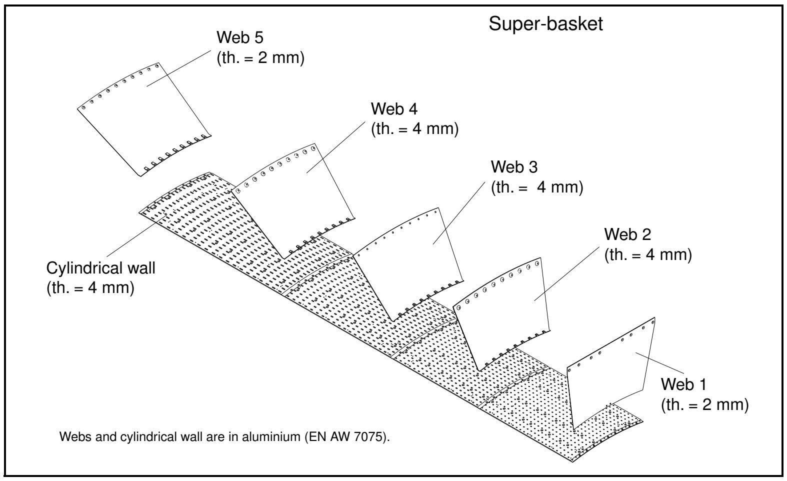

Fig.1.3: The super-basket

1.3 The Method

Building an FE-model of the basket is rather easy. By contrast simulating the complex assembly of the sub-modules with the grid and the super-basket would be difficult. For that reason we have developed a sequential method that performs and combines simple steps including experiments, FE-models, and computing iterations.

i Prototype sub-modules are connected together in packages and deformations measured for unsupported loading conditions, providing the stiffness of the packages with respect to their self-weight.

ii Prototype sub-module packages are connected to the reduced basket and deformations measured for the typical loading conditions.

iii An FE-model only representing the reduced basket stiffness is built to compute deformations for the typical loading conditions, providing the stiffness of the reduced basket with respect to the supported load.

iv A combination of the above inputs taking inelastic displacement on account results in stiffness parameters for the sub-modules with respect to the relevant loading conditions, i.e. under combined self-weight and reaction forces from the end support, and thereby the transmitted forces to the reduced basket.

v Repeating steps **iii** and **iv** for a new version of the basket design (super-basket) provides the transmitted forces to the modified support.

vi The transmitted forces are applied in the FE-model for the super-basket in interaction with additional relevant load cases, and analyses are performed to validate the new design.

2 Geometry and Finite Element Models

2.1 Reduced Basket FE-Model for Stiffness Analysis

We model for an FE-analysis the reduced basket used to support a fraction of the load of sub-modules (The sub-modules load is about 490 kg). We compare the results of this FE-analysis in 3 oÕclock position with the experimental results obtained on a prototype test assembly by conventional measurements (dial gauges) and photogrammetry. This analysis produces an input for step **iv** in 1.3.

The basket consists of the 2mm-thick front and rear cones and the 4mm-thick cylindrical wall. The basket is connected to the grid with 10 screws by its front and rear cones. At their cantilevered end the 10 sub-modules of each type are connected together to form 1 package (4 packages in total). The second and the eighth sub-module in each package are connected with the basket cylindrical wall each by 2 Set-Pins (Fig.2.2.a), resulting in 2 rows of 8 set-pins (16 set-pins in total). We try to be as close as possible to reality in the definition of the geometry of this FE-model (Fig.2.1.a). During meshing, we divide the 3 walls into elements with different sizes in order to obtain nodes close to the real connection points on the prototype test assembly. The front, rear and cylindrical walls are modelled with shell elements. For the cylindrical wall, perforated by a large number of oval holes for optical fibres and by set-pin holes for sub-modules, equivalent orthotropic stiffness parameters are obtained by unit cell analyses [1] and are assigned to the elements.

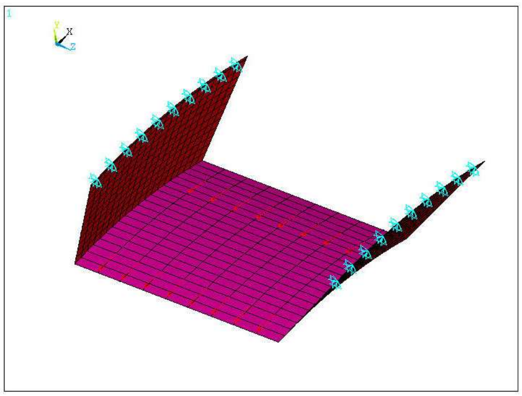

(a) The reduced basket

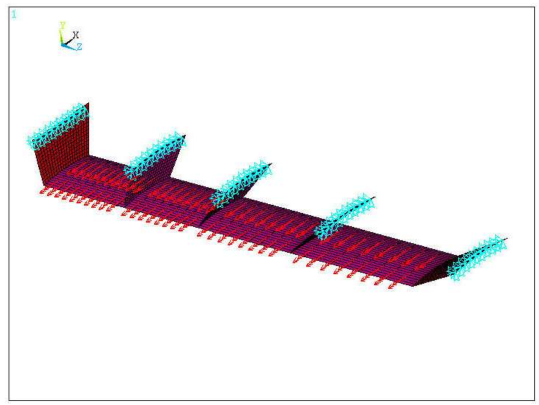

(b) The super-basket

Fig.2.1: FE-Models

Type of elements used:
ANSYS Shell 181, 4 nodes, hybrid-mixed shell elements with incompatible modes and full integration.

Applied units:
Length [mm], Mass [g], Force [N].

Type of materials used:
Rear and front conical walls (Aluminium EN AW 5083)
$E = 69500$ $\nu = 0.33$ $\rho = 0.0027$

Cylindrical wall (Aluminium EN AW 5083, equivalent parameters for perforated plate)
$Ex = 57727$ $Ey = 49540$ $Ez = 63940$
$Gxy = 19518$ $Gyz = 24006$ $Gxz = 24006$
$\nu xy = 0.3434$ $\nu yz = 0.2559$ $\nu xz = 0.2981$ $\rho = 0.002453$

Constraints and loads:
Screws connecting basket and grid are modelled by constraining all translations. As reference load a force of 1 N in x direction (in the super-module local coordinate system) is applied to each node provided at the location of a set-pin connecting the sub-modules and the cylindrical wall, i.e. 16 N for the entire model.

2.2 Set-Pin Geometry, Stresses and Displacements

Fig.2.2.a represents the set-pin geometry, that provides a degree of freedom in y direction while transmitting forces in x and z directions. Fig.2.2.b represents the major part of inelastic displacement (0.07 mm) due to adjustment tolerances between dowel and cylindrical wall. We assume that the set-pin is like a beam embedded in the sub-module insert with a reaction force in the region of contact between the set-pin and the cylindrical wall (Fig.2.2). Assuming that about one third of the sub-modules load is taken by the set-pins, four rows of set-pins connecting the sub-modules to the cylindrical wall gives a safety factor of 1.5 against material yield in the set-pins, and the computed maximum displacement at the set-pin end is 0.0146 mm. This number of four rows is retained for the super-basket design.

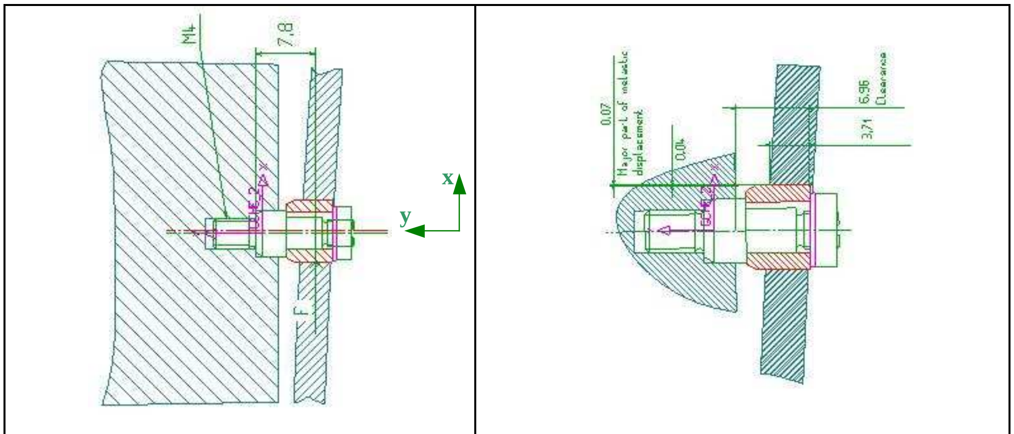

(a) Applied set-pin force **(b)** Set-pin geometry and displacements

Fig.2.2: Set-pin design

2.3 Super-Basket FE-Model for Stiffness Analysis

In the second phase of the simulation (step **v** in 1.3), we model the entire super-module conical and cylindrical walls, called super-basket. As for the previous model, we take all the constraints in account for a realistic modelling of the super-basket in FE (Fig.2.1.b).

The two end walls are 2mm-thick, the three others conical walls (middle) and the cylindrical wall are 4 mm-thick to stay within the geometrical envelope. As for the previous model, during the meshing the different walls are divided in elements with different sizes so that nodes on the FE-model are close to the connection points in the real assembly. The different walls are all modelled with shell elements.

Type of elements and materials used:
The same elements and material properties are used as in the first model. The same equivalent parameters for perforated plate are taken. The value of the stiffness parameters found for the 4 sections of the cylindrical wall is averaged to simplify the model.

Constraints and loads:
Screws connecting basket and grid are modelled as in the previous model by constraining all translations. As reference load a force of 1 N in x direction (in the super-module local coordinate system) is applied to each node provided at the location of a set-pin connecting the sub-modules and the cylindrical wall, i.e. 136 N for the entire model (Four rows of set-pins are used according to 2.2 with respect to admissible stress for the set-pins).

2.4 Super-Basket FE-Model for Static Analyses

The FE-model for static analyses is the same as in the previous case (Fig.2.1.b). The relevant load cases for the analyses are the weight of the sub-module packages in 3 or 9 oÕclock position as well as an imposed displacements resulting from a positive or negative Off-Plane of one of the super-module supporting points with respect to the other three (Fig.1.1.b) due to inaccuracies in production. Constraints and loads are changed for the 4 different following cases:

a) 3 oÕclock position with positive off-plane
b) 3 oÕclock position with negative off-plane
c) 9 oÕclock position with positive off-plane
d) 9 oÕclock position with negative off-plane

Constraints and loads:
For all load cases displacements of the fixation points of the super-basket to its support (known from previous analyses) are imposed to the first (flat), second, third and fifth (conical) walls, while the fourth wall is taken as a reference. In addition, for the weight load forces of 55.8 N per set-pin obtained in step **v** were applied:
3 oÕclock position:
Imposed fixation displacements under 3 oÕclock loading, 55.8 N opposite to x direction.

9 oÕclock position:
Imposed fixation displacements under 9 oÕclock loading, 55.8 N in x direction.
Positive off-plane:
Imposed fixation displacements under imposed positive off-plane.
Negative off-plane:
Imposed fixation displacements under imposed negative off-plane.

The force of 55.8 N in –x direction (in the super-module local coordinate system) is applied to each node provided at the location of a set-pin connecting the 4 rows of sub-modules and the cylindrical wall, i.e. 7589 N for the entire cylindrical wall.

3 Analyses and Results

3.1 Model for Analysis Delivering Stiffness and Loading

In order to estimate the participation of the super-basket in supporting the module weight, the stiffness properties of both the super-basket and the sub-module packages are needed. The stiffness of the super-basket was obtained by evaluation of its FE-model (step **v** in 1.3). For the sub-module packages, representing a highly complex structure, available experimental data combined with a simple FE-model of the reduced basket were used (steps **i** to **iv** in 1.3) to deliver their stiffness with respect to their self-weight as well as to the support reaction acting at the level of the set-pins. Fig.3.1 schematically illustrates the method. In a first test (step **i** in 1.3) cantilevered sub-module packages (without reduced basket) are loaded by their self-weight (G) and the resulting end deflection U_1 is measured. This provides the stiffness C_G of the sub-module packages with respect to loading G:

$$U_1 = G / C_G \qquad (1)$$

For the second test (step **ii** in 1.3) the reduced basket is mounted, the assembly is brought to the same position and again the resulting end deflection U_2 is measured. For this loading the following relations hold:

$$U_2 = G / C_G - F_2 / C_F \qquad (2)$$

$$U_2 = \Delta U + U_w = \Delta U + F_2 / C_w \qquad (3)$$

where F_2 is the force transmitted between the package end and the reduced basket, C_F is the stiffness of the package with respect to loading at its end in x-direction, C_w is the stiffness of the reduced basket with respect to loading in x-direction and U_w is the end deflection of the reduced basket. ΔU represents an inelastic relative displacement between the sub-module ends and the basket due to the clearance between the two parts, inelastic deformations of the set-pins, inelastic displacements at web fixation points to the grid, etc.

Subsequently, the reduced basket (without sub-module packages) is modelled by finite elements (see 2.1) and the set-pin locations on the cylindrical wall (2 rows of pins analogous to the 2nd test) are uniformly loaded in x-direction (F_3). The resulting set-pin displacement U_3 provides a value for the stiffness of the reduced basket (step **iii** in 1.3):

$$U_3 = F_3 / C_w \qquad (4)$$

Aside from ΔU, linear elastic behaviour of all components is assumed. Other implicit assumptions are uniform stiffness properties for all types of sub-module packages, as well as uniform (along z-axis) load distribution and uniform deflection in the cylindrical wall of the super-basket and the reduced basket. Therefore each loading, displacement and stiffness property can be represented by one single value.

To summarise, the input quantities for the above equations are the loads G, F_3 and the displacements U_1, U_2, U_3, ΔU, which deliver the stiffness parameters and the transmitted load to the reduced basket as output (step **iv** in 1.3), i.e. C_G, C_F, C_w and F_2. Since G represents a distributed load with the centre of gravity located near half the length of the sub-modules, while F is a concentrated load acting at their free ends, one can expect the following relation between C_F and C_G to hold which represents a constraint on the input values:

$$C_F \leq C_G / 2 \qquad (5)$$

The input values applied are the following:
$G = 4800$ N Éknown module weight
$U_1 = 0.660$ mm ; $U_2 = 0.150$ mm Éaveraged values from measured data

$F_3 = 16$ N ... chosen reference load
$\rightarrow U_3 = 0.0005$ mm ... delivered by FE-analysis (see Fig.3.2)

With regard to the existing clearances in the front set-pin system resulting in an inelastic displacement of about 0.07mm (see 2.2 and Fig.2.2) the total amount of ΔU is estimated to be smaller than 0.1 mm. On the other hand, given the input values G, F_3, U_1, U_2 and U_3 for equations (1) to (4), equation (5) requires ΔU to be greater than 0.092 mm. Hence the following value is chosen:
$\Delta U = 0.095$ mm

Finally the output values become:
$C_G = 7273$ N/mm ; $C_F = 3451$ N/mm ; $C_w = 32000$ N/mm ; $F_2 = 1760$ N

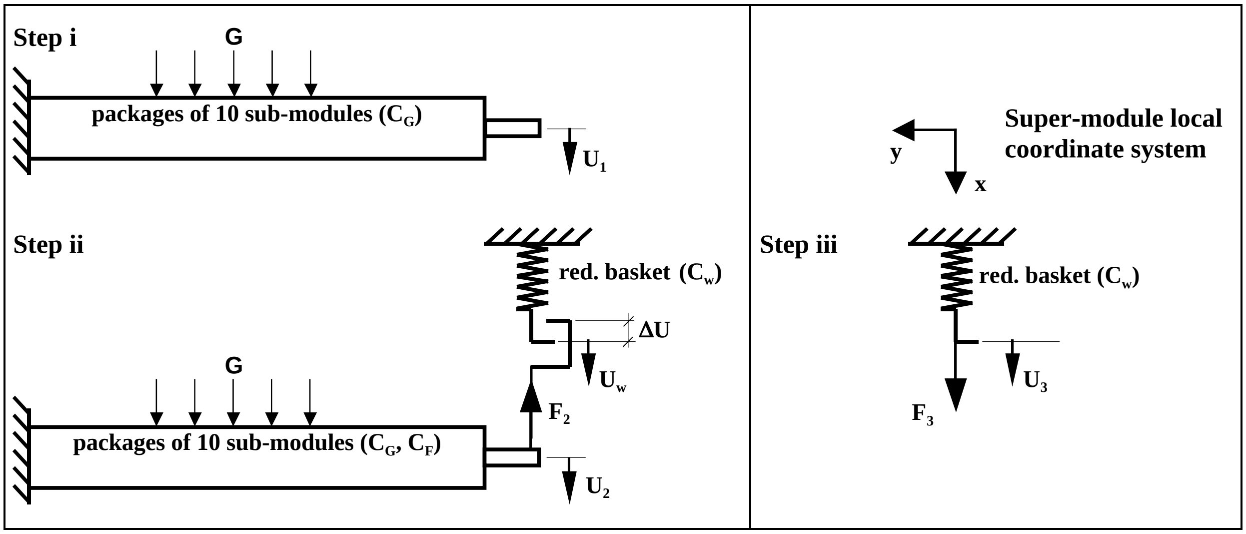

Fig.3.1: Simplified model for sub-module packages and reduced basket

Now for the full super-module (step **v** in 1.3) the weight and the stiffness parameters of the sub-module packages can be assumed to change proportionally with their number, i.e.:
$G_{full} = 17/4\ G = 20400$ N ; $C_{G,full} = 17/4\ C_G = 30910$ N/mm ; $C_{F,full} = 17/4\ C_F = 14667$ N/mm
=> $U_{1,full} = U_1 = 0.660$ mm

Also ΔU can be assumed to remain unchanged, i.e.:
$\Delta U_{full} = \Delta U = 0.095$ mm

However, the stiffness of the full super-basket $C_{w,full}$ and hence its contribution to supporting the sub-modules $F_{2,full}$ are still unknown. In an analogous approach as for the reduced basket equations (1) to (4) can be rewritten for the full super-module:

$$U_{1,full} = G_{full} / C_{G,full} \tag{6}$$

$$U_{2,full} = G_{full} / C_{G,full} - F_{2,full} / C_{F,full} \tag{7}$$

$$U_{2,full} = \Delta U_{full} + F_{2,full} / C_{w,full} \tag{8}$$

$$U_{3,full} = F_{3,full} / C_{w,full} \tag{9}$$

In order to find $C_{w,full}$ from equation (9) an FE-model of the full super-basket was made (see 2.3 and Fig.2.1.b), uniformly loaded in x-direction ($F_{3,full}$) at set-pin locations (4 rows of set-pins, see Fig.3.2.b) and the resulting displacements at these locations were averaged ($U_{3,full}$):
$F_{3,full} = 136$ N $\rightarrow U_{3,full} = 0.00085324$ mm
=> $C_{w,full} = F_{3,full} / U_{3,full} = 159392$ N/mm

$C_{w,full}$ turns out to be higher than 17/4 C_w, which means that the super-basket would support a higher ratio of the load than the reduced basket. Finally $F_{2,full}$ can be found from equations (6) to (8):

$$F_{2,full} = (U_{1,full} - \Delta U_{full}) / (1 / C_{F,full} + 1 / C_{w,full}) \tag{10}$$

With the values provided above the nominal total load on the super-basket in 3 oÕclock position becomes:

$F_{2,full}$ = 7589 N or **55.8 N/pin** (for assumed 136 set-pins) (11) which is slightly higher than 17/4 F_2 in accordance with the stiffness parameters of the super-basket compared to the reduced basket. $F_{2,full}$ is assumed to be evenly distributed among the set-pins.

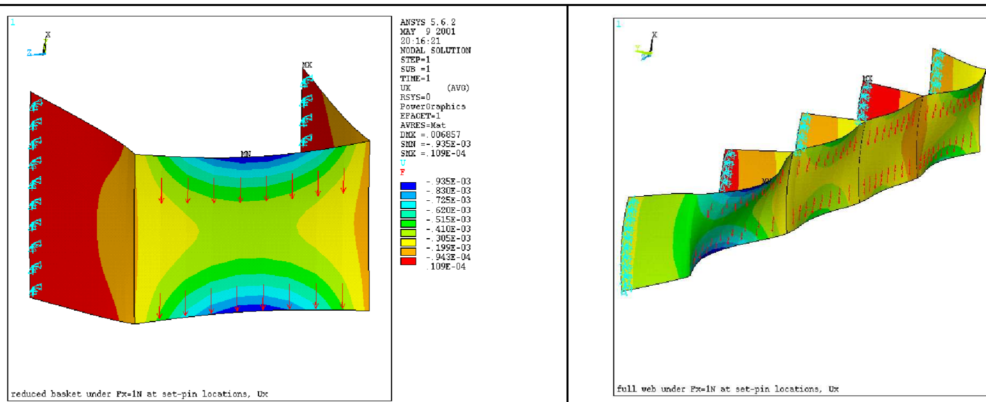

(a) Reduced basket: 16 set-pins **(b)** Super-basket: 136 set-pins

Fig.3.2: Tangential displacements Ux for Fx = 1 N per set-pin

For the buckling analysis the load factor λ_G is of interest, by which the total weight of the sub-modules G_{full} must be increased in order to initiate buckling. On the other hand, since the sub-module packages are not present in the FE-model, only a buckling load factor λ_F for $F_{2,full}$ can be computed, which is not the same as λ_G. The relation between the two load factors can be obtained from equation (10) considering that λ_F and λ_G would apply to $F_{2,full}$ and $U_{1,full}$ respectively while ΔU_{full} would remain unchanged:

$$\lambda_F F_{2,full} = (\lambda_G U_{1,full} - \Delta U_{full}) / (1 / C_{F,full} + 1 / C_{w,full}) \geq 0 \qquad (12)$$

For the actual values the above equation leads to:

$$\lambda_F = 1.168\,\lambda_G - 0.168 \geq 0 \quad \text{or} \quad \lambda_G = 0.856\,\lambda_F + 0.144 \geq 0.144 \qquad (13)$$

3.2 Static Analyses and Results for Super-Basket

As mentioned in 2.4 the load cases considered are the super-module weight in 3 and 9 o'clock, each combined with 0.3 mm imposed off-plane to the super-module support in either positive or negative direction.

Two linear static analyses were performed in order to obtain the displacement, stress and force responses to the above load cases. In the first one (3 o'clock) $F_{2,full}$ from (11) was applied to the cylinder and boundary conditions for 3 o'clock were applied to the webs. In the second one (off-plane) only the boundary conditions for off-plane were applied to the webs. Subsequently, the responses were combined at nodal level as follows:

$$R = \gamma_{G,p} |R_{3oc}| + |R_{off}| \qquad (14)$$

where R_{3oc} and R_{off} are the responses to the load cases 3 o'clock and off-plane respectively, $\gamma_{G,p} = 1.35$ is the safety factor for permanent loads in persistent design situations [2] and R is the total response to the worst combination of either of the 3 or 9 o'clock cases with either of the off-plane cases in the positive or negative direction. In accordance with [3] also Von Mises stresses were conservatively combined using (14).

In equation (14) the inelastic displacements ΔU are neglected. Otherwise for the load case 3 o'clock the load safety factor $\gamma_{G,p} = 1.35$ would only apply to the imposed boundary conditions, while consistent with (13) the load safety factor for the forces acting on the cylinder ($F_{2,full}$) should be calculated as: $\gamma_{F,p} = 1.168\,\gamma_{G,p} - 0.168 = 1.41$. Hence, neglecting ΔU is equivalent to underestimating these forces by about 4%.

In the buckling analyses the weight load at ±(3 o'clock) is considered as variable while the parameter load (off-plane) can vary independently between ±0.3 mm. Here the inelastic displacements ΔU are also taken into account. A detailed description of the iterative algorithm used to obtain the minimum buckling load factor under the worst loading condition is presented in [4].

Results of the static analyses are summarised in tables 3.1 to 3.3:

The *joint forces* in table 3.1 are the nodal force and moment components transmitted between the webs and the cylinder at their joints, where the whole length of each joint is modelled by 21 nodes. The nodes with maximum values of each force or moment component are listed. The highest forces appear in the 2nd and the 4th web.

The *screw forces* in table 3.2 refer to the nodal reaction forces at the locations of the screws fixing the webs to the grids, the distribution of which can be seen in Fig.3.3.a. These are also forces per node, where each screw is modelled by one node. Again the nodes with maximum values of each force component are listed. The highest forces appear in the 2nd and the 4th web with their extreme values within one web being at the sides.

Maximum displacement components, maximum Von Mises stress and minimum buckling load factor are listed in table 3.3, and displacement distributions are shown in Fig.3.3. Extreme displacement values for each node can occur under a different load case combination, and displacements are reversed for opposite load cases, while in the figures the absolute values are shown. Therefore the deformed shape in these figures does not bear any meaning. Extreme values of the Von Mises stress appear at singularities in the FE-model near the locations of the side screws in the 2nd and the 4th web resulting from the high reaction forces there. Their actual values depend on details of the bolted joint. Buckling modes in all analyses appear in the thinnest (1st or 5th) or in the most loaded (2nd or 4th) webs. The first mode under the worst conditions appears in the 1st (flat) web.

node / web	Fx [N]	Fy [N]	Fz [N]	Mx [Nmm]	My [Nmm]	Mz [Nmm]
368 / 2	**490.0**	2.3	1.2	22.5	0.6	7.7
348 / 2	115.3	**38.0**	11.1	64.7	10.4	1.7
1334 / 4	163.6	28.4	**53.2**	154.3	**26.4**	3.3
360 / 2	203.6	15.0	8.5	**163.6**	24.2	3.6
1826 / 5	150.1	0.3	1.8	22.5	8.2	**19.2**
total average	162.1	10.2	8.1	73.1	10.2	5.4

Table 3.1: Load case comb. 1.35 × |3 o'clock| + |off-plane|, maximum joint forces

node / web	Fx [N]	Fy [N]	Fz [N]
627 / 2	**1114**	2035	795
861 / 2	990	**2374**	935
1794 / 4	610	1636	**2145**
total average	420	459	354

Table 3.2: Load case comb. 1.35 × |3 o'clock| + |off-plane|, maximum screw forces

Ux [mm]	Uy [mm]	Uz [mm]	σ_{VM} [MPa]	$\lambda_{F,min}$
0.591	**1.618**	**0.283**	**30.480**	**3.143**

Table 3.3: Load case comb. 1.35 × |3 o'clock| + |off-plane|, maximum displacements, maximum Von Mises stress and minimum buckling load factor

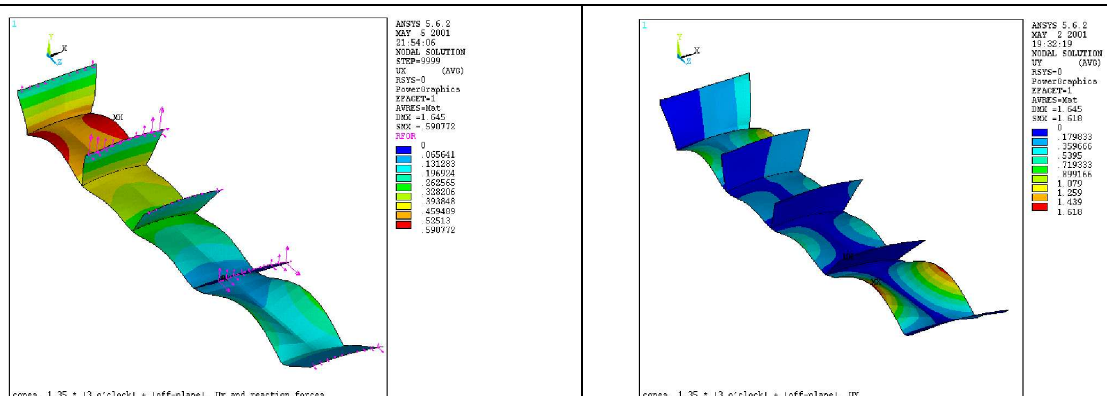

(a) Tangential displacements Ux and screw forces **(b)** Radial displacements Uy

Fig.3.3: Load case comb. 1.35 × |3 o'clock| + |off-plane|

4 Conclusions: Solutions Brought by the Design Revision

4.1 The Super-Basket Concept

The CMS project planning constraints did not give time for performing tests on the most critical structural elements (sub-module packages) on a sufficient time scale to extrapolate to the experiment life-time, and in turn to accept a dominantly cantilevered structure. The load share put on materials and connections potentially subject to creeping was therefore minimised. The super-basket design is solidly assessed by the sequence of tests proofing each building element, and by computations that represent the mechanism of interaction between elements, at the model scale as well as at full scale.

4.2 The Super-Basket Design Performance

Computations forecast a sag reduction at 3 o'clock from 0.66mm to 0.15mm. At 3 o'clock with an overload of 35% complying with EUROCODE [2, 5] safety factors*, and with a 0.3mm off-plane maximal error from the super-module fixation, the overall stress level is lower than 30MPa to compare with the selected alloy (EN AW 7075) yield strength 350MPa (second web). Needless to say, the building elements selected material and computed dimensions do not impair the physical performance of the Calorimeter.

4.3 The Super-Basket Construction

The technological problems of the connections, production and assembly optimal condition have been resolved. The super-basket is made of one cylindrical wall and five webs, assembled by screws (Fig.1.3).

The **Cylindrical Wall** is a 4mm-thick EN AW 7075 plate that covers the super-module front part. It provides the holes to locate the four rows of set-pins required to cantilever the sub-modules.

The **Webs** connect the cylindrical wall to the grids and support most of the cantilever moment. The first and fifth webs are 2mm thick, the second, third and fourth ones are 4mm thick. They are made of EN AW 7075 alloy too. The first web is flat, whereas the four others are conical.

The **Screwed Junctions.** Each web is screwed to the grid and to the cylindrical wall, making the super-basket assembly a conventional operation. Nevertheless, because of the calorimeter compactness the screwed junctions are carefully dimensioned and specific calculations are derived from the computed reaction forces (boundary conditions) and from the efforts given at the nodes. All screws are made of austenitic steel, class 70, quality A2, diameter M6, conical-headed, with an adjusted 8mm rod to take dominant shear forces of the cantilever.

Because of their complex shapes, wall and webs are produced by 4-axes CNC milling. Machining from solid plates is possible with the selected EN AW 7075 tension-free alloy. In spite of the important material loss, it is preferred to a complex sequence of forming, welding or riveting, tempering and finishing.

5 References

[1] H. Rezvani Naraghi: *CMS ECAL Barrel, Unit Cell Analysis for Basket Bottom Plate*, CMS Note 1999/049, CERN, Geneva, 1999.

[2] Eurocode 3: *Design of Steel Structures, Part 1.1: General Rules and Rules for Buildings*, European Prestandard, ENV 1993-1-1, CEN (European Committee for Standardization), Brussels, April 1992.

[3] H. Rezvani Naraghi: *CMS ECAL Barrel, The Worst Combination of Loads*, CMS Note 2000/051, CERN, Geneva, 2000.

[4] H. Rezvani Naraghi: *A New Algorithm for Buckling Analyses under Non-Proportional Loading — with Application to CERN CMS Experiment*, in H. A. Mang, F. G. Rammerstorfer, J. Eberhardsteiner, Eds., Proc. 5th World Congress on Computational Mechanics, WCCM V, Vienna, July 2002.

[5] Eurocode 8: *Design Provisions for Earthquake Resistance of Structures, Part 1.1 / 1.2: General Rules — Seismic Actions and General Requirements for Structures / General Rules for Buildings*, European Prestandard, ENV 1998-1-1 / ENV 1998-1-2, CEN (European Committee for Standardization), Brussels, April 1994.

* Because of the super-module structural stiffness (high frequency response) this static load also covers the seismic equivalent load.